

**Research Article**

# PTX Inhibits Migration and Inflammatory Mediators in MCF-7 Breast Cancer Cells

**Kriti Bhardwaj<sup>1</sup>, Karishma Niveria<sup>2</sup>, Vinay Kumar Singh<sup>1</sup>, Anita Kamra Verma<sup>2,3\*</sup>, Kapinder<sup>1,4\*</sup>**

<sup>1</sup>Department of Zoology, Deen Dayal Upadhyaya Gorakhpur University, Gorakhpur, U.P., India

<sup>2</sup>Nanobiotech lab, Kirori Mal College, University of Delhi, 110007, Delhi, India

<sup>3</sup>Fellow, Delhi School of Public Health, Institution of Eminence, University of Delhi, India

<sup>4</sup>Department of Zoology, University of Allahabad, Prayagraj, U.P., India

**\*Corresponding authors:** Anita Kamra Verma, Nanobiotech lab, Kirori Mal College, University of Delhi, 110007, Delhi, India.

Kapinder, Department of Zoology, Deen Dayal Upadhyaya Gorakhpur University, Gorakhpur, U.P., India.

**Citation:** Bhardwaj K, Niveria K, Singh VK, Verma AK, Kapinder (2024) PTX Inhibits Migration and Inflammatory Mediators in MCF-7 Breast Cancer Cells. Curr Res Cmpl Alt Med 8: 253. DOI: 10.29011/2577-2201.100253

**Received Date:** 18 September 2024; **Accepted Date:** 23 September 2024; **Published Date:** 26 September 2024

**Abstract**

**Background:** Paclitaxel (PTX) potentially inhibit mitosis is extremely effective in the breast cancer treatment. However, metastatic potential and resistance development of breast cancer cells to PTX limits its clinical use. Although the specific machinery of PTX cytotoxicity is still controversial, stabilization of microtubule is well-thought-out the main mode of action of PTX. **Objective:** To explore effects of PTX and HEX on proliferation and migration of breast cancer MCF-7 cell line. **Methodology:** Alterations in cellular morphology was done by Scanning electron microscopy (SEM) cell viability of MCF-7 cells was estimated by methyl thiazolyl tetrazolium (MTT) assay. MCF-7 cell migration was tested with transwell migration assay. Cytokine levels induced by PTX were assessed by ELISA. **Results:** Compared to the control group, MCF-7 cell viability was significantly reduced by PTX and HEX, and the inhibitory rate was highest at 48 h ( $P < 0.05$ ). MCF-7 cell migration was significantly inhibited in paclitaxel. Moreover, in comparison to the control group, the number of MCF-7 cells. PTX inhibited the migratory potential of MCF-7 breast cancer cells and significantly decreases IL-10 expression. PTX retarded the migratory potential and inflammatory mediator production which delivers an experimental root for the probable application in the breast cancer treatment. **Conclusions:** These results suggested PTX could inhibit proliferation and migration in breast cancer MCF-7 cells and also serve as an anti-inflammatory and immune modulator.

**Keywords:** Paclitaxel; Breast cancer; Immune modulator

## Introduction

Paclitaxel (PTX) marketed name of Taxol is a tricyclic diterpenoid composite naturally extracted from the needles and bark of *Taxus brevifolia*. The molecular formula written [1] as  $C_{47}H_{51}NO_{14}$ , and its chemical structure is shown in Fig. 1.

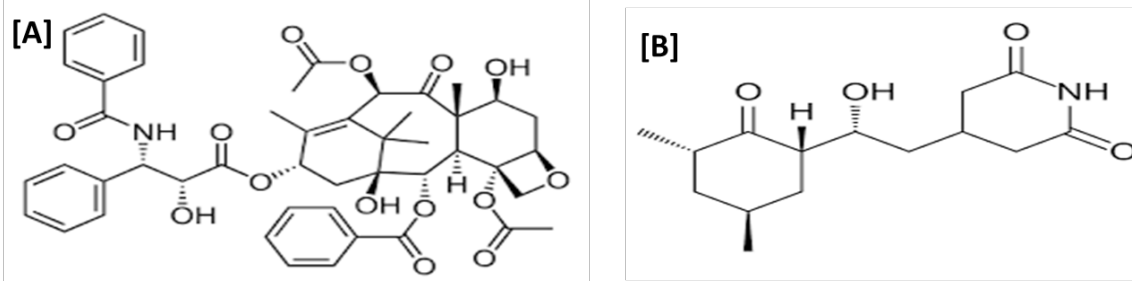


**Figure 1:** Structure of [A] Paclitaxel (PTX) and [B] Cycloheximide (HEX).

PTX is frequently used in treatment of cancer due to its extraordinary antitumor effectiveness [2-4]. Even though PTX has been widely studied in the arena of oncology, scientists have discovered that PTX also applies healing properties on non-neoplastic diseases, such as vascular diseases, fibro-proliferative diseases, and inflammatory diseases [5,6]. PTX-stabilized microtubules may hinder with cellular mitosis, ultimately leading to programmed cell death (apoptosis). PTX endorses the tubulin assembly and microtubules formation and prevents the detachment of microtubules, prevention of mitosis, blockage of cell cycle and inhibiting spread and division of the cancer cells [7]. It is also used in axon regeneration, inflammation, renal and hepatic fibrosis, skin disorders, coronary heart disease, and clinical trials are being conducted for degenerative brain diseases [8].

Cycloheximide is a *Streptomyces griseus* derived small molecule which initially functions as fungicide. HEX is reported as ribosome inhibitor, restricts translation elongation in protein synthesis [9]. HEX itself made some protector proteins which causes imbalance of the proteins and leads to apoptotic mode of cell death. This molecule also involved TNF- $\alpha$  secretion in cell-specific range causing apoptosis. HEX also involved in activation of muscle glucose transport as well as in fibroblasts and 3T3-L1 adipocytes [10].

Breast cancer is the most regularly spotted cancer and the foremost source of cancer-related death amid females globally with an estimated incidence of 2.3 million new cases in 2020 [11]. Presently, ordinary therapies for breast cancer patients include surgical procedure, radiation and chemotherapy, which governs an inimitable role [12]. PTX, a first-line treatment in clinics to treat breast cancer that employs its antineoplastic commotion by encouraging the polymerization of tubulin and steadying the subsequent micro-tubules, leading to cell cycle detention at the

G2/M phase that stimulates apoptosis in cancer cells.

Cytokines, are tiny proteins secreted from numerous types of cells, convey precise functions on cell phenotype through cell to cell contact messaging [13]. Inside of tumor microenvironment, ascites has been enclosed by lymphocytes, stromal cells, and extracellular matrix, immune cells, and blood vessels, etc. [14]. Cytokines generally attentive the immune cells towards any kind of damage of tissue and the infection persistent. But persistent production of cytokines at ant site of body could, in chance, trigger immune cells to further conceal cytokines that may act as both in paracrine and autocrine manner causing a state of chronic inflammation that promotes cancer proliferation [15]. Parenthetically, the tissue damage leads to the generation of inflammatory response possesses signaling cascades with carcinogenesis that include induction of cell proliferation and blood vasculature [16]. In the tumour micro-environment (TME), cytokines reduce the anti-tumor immunity of cells and generate a tumor-supportive microenvironment that directly exerts a tumor-promoting signals [17]. This process may appear to occur locally, but the cytokines secreted at the TME also had own biological roles which mediated via circulation hence supported in tumor metastasis. This chronic-inflammatory situations can be enhanced by other supporting conditions involving cigarette smoking, alcohol consumption, excess body fat, sedentary lifestyle, and chronic infections that excite systemic inflammation of lower-grade [18]. The systemic inflammation further quickens progression of cancer by altering the TME dynamics persuading an additional cancer-promotive environment [15]. Numerous anti-cancer therapies including chemotherapy, radiation therapy, and although recently invented biologic therapies and immunotherapies could persuade elimination of cancer cells leading to potentiate inflammation. The inflammation that encourages robust immune responses might be advantageous

for anti-tumor immunity. Moreover, certain immune-stimulatory cytokines might not be advantageous for cancer treatment and may involuntarily enhance tumor regrowth or causing immune-suppression. IL-4 and IL-10 secretion of cytokines by tumor ascites has been shown to cause drug-induced resistance, by specifically inhibiting cellular programmed death. Therefore, PTX induced cytokines TNF- $\alpha$  and IL-10 were assessed as they are in systemic inflammation and is accountable for the lively balance of apoptosis and survival pathways.

## Material and methods

### Chemical reagents:

MCF-7 cell line was procured from NCCS pune, PTX were purchased from Sigma-Aldrich. MTT, a tetrazolium yellow coloured salt was purchased from Sigma-aldrich Co., (St. Louis, MO, United States). Fetal bovine serum (FBS) was procured from GIBCO. Dimethyl sulphoxide (DMSO), Glutaraldehyde (25% v/v), and Ethanol were purchased from SRL Pvt Ltd. India. Trypsin, Antibiotic solution streptomycin and penicillin, Dulbecco's modified Eagle's medium (DMEM) were procured from HiMedia Pvt Ltd. All other chemicals were of analytical grade and obtained from Merck India Ltd. (Mumbai, India).

**Cell Viability Assay:** MCF-7 cells were maintained in DMEM added with 10% FBS and 1% strept-penicillin antibiotic in CO<sub>2</sub> incubator maintained at 37°C and 5% CO<sub>2</sub>. Viability of cells was evaluated using MTT assay. 5 $\times$ 10<sup>3</sup> cells/well seeded in 96-well plates and placed in CO<sub>2</sub> for overnight in DMEM and added with 10% FBS. Cells were treated with different concentrations of PTX (12.5  $\mu$ g/mL, 25  $\mu$ g/mL, 50 $\mu$ g/mL and 100 $\mu$ g/mL) or HEX (12.5  $\mu$ g/mL, 25  $\mu$ g/mL, 50 $\mu$ g/mL and 100 $\mu$ g/mL) in serum-free conditions were evaluated as modified protocol [19]. The control group contained cells incubated in no FBS supplemented medium. Afterwards completion of 48 h, 20  $\mu$ l MTT (5 mg/ml) solution was added to each well and stored in CO<sub>2</sub> incubated for 4 h causing formation of formazan crystals at 37°C followed with addition of 150  $\mu$ l DMSO to each well and further incubated at 37°C for 30 minutes. The coloured intensity of viable cells forming formazan crystals were recorded in terms of optical density using a ELISA microplate reader (USCN Life Sciences, Wuhan, China) at 570 nm. All experiments were accomplished in triplicates and the results were presented as the proportions related to the controls.

Percent viability of the cell was determined using equation:  
**100 – % Cytotoxicity.**

Where Percent cytotoxicity was calculated as follows

$$\frac{\text{Absorbance of the control sample (A)}_c - \text{absorbance of the sample to be tested (A)}_t}{\text{Absorbance of the control sample}} \times 100 \quad \dots \dots \dots \text{(i)}$$

where, [A]<sub>c</sub> = Absorbance of the control sample; [A]<sub>t</sub> = Absorbance of the sample to be tested.

### Morphological assessment of cell by SEM

The morphological structure of breast cancer cell line has been recorded throughout the experimental set up to observe any kind of contaminants. The morphological changes due to exposure to drug concentration and possible distortion at the membrane layer has been recorded using SEM. This technique uses the electron interaction with the sample object which provide information about surface morphology, chemical configurations and exterior layers. The signal generated by this has been recorded by the computer monitor and analysed using specific software. The working principle involves generation of a strong electron beam using electron gun which organised by a group of lenses to make an upright path through the microscope to strike on the surface of the sample. After the strike, electrons and x-rays has been emitted from sample. By using the sensors to assemble these rays to generate a 3-D image of the object. Result was analysed using JEOL Japan Mode: JSM 6610LV which functioned at 1-30kV. For dispersing of object, double-sided tape coated with Aluminium stubs has been used. Then the object surface has been bombarded

with gold and after that observe under the microscope.

MCF-7 cells were seeded at 5 $\times$ 10<sup>6</sup> density in 24 well plate over the 12mm coverslips, and positioned in a CO<sub>2</sub> incubator for the overnight. Afterwards, PTX (~8.56 $\mu$ g/mL) and HEX (~26.5  $\mu$ g/mL) treatment has been given for 18 hrs followed by cell fixation using 4% paraformaldehyde (PFA) for 30 min. Cells were splashed twice using PBS (pH 7.4) to remove excesses traces of PFA. For SEM, cell dehydration has been done using gradual increasing concentration of alcohol. For each gradient, 5 min. of exposure has been given to the cells till the absolute alcohol then processed for SEM imaging.

### Scratch Assay

A scratch assay was used to assess cell migration. MCF-7 of density 5 x 10<sup>6</sup> cells/well were seeded in 6-well plates. When the cells attained more than 90% confluence, they were injured using autoclave pipette tips. The detaching cells were lightly washed using PBS. After exposure to PTX (~8.56 $\mu$ g/mL) and HEX (~26.5  $\mu$ g/mL), the injured parts were photographed immediately using

a microscope and healing has been recorded at 24 hrs (IX51; Olympus, Japan) and the migratory potential of cells was analysed (Faria et. al 2021). Experiments were repeated in triplicate independently. Percent wound closure was calculated using the following equation:

$$\text{Percent wound closure (\%)} = [1 - (L_t/L_0)] \times 100\% \dots \dots \dots \text{(ii)}$$

### Transwell-migration and invasion assay:

To study the potential of MCF-7 cells to metastasize, the classic transwell assay were performed. Cultured MCF-7 cells were treated with PTX (~8.56 $\mu$ g/mL) and HEX (~26.5  $\mu$ g/mL). Post 48 hours of incubation of the untreated control group, PTX group and HEX group cells were trypsinized, and centrifuged to collect the cell density and resuspend the cells into DMEM media with no FBS. For performing migration assay,  $2.5 \times 10^5$  cells/well seeded on the top 6-well inserts (8  $\mu$ m pore size, 6.5 mm dia.). FBS supplemented DMEM medium were used as chemoattractant to create the gradient. The lower well carefully filled so that, it touched the polycarbonate membrane in the upper inserts. Transwell plated cells were placed in CO<sub>2</sub> incubator for 12 hrs, and the upper chamber DMEM media having non-migrated MCF-7 cells were removed using a cotton bud. For invasion assay, the transwell membranes were first coated with a thin layer of Matrigel and left overnight at 4 °C. Subsequently,  $5 \times 10^5$  cells /well were seeded into Matrigel-coated transwell inserts and the lower wells were filled with DMEM medium containing 10 % FBS. Cultured MCF-7 cells were exposed to HEX and PTX for 18 hrs. After 18 hr, the non-invaded cells and the Matrigel in the upper chamber were gently swabbed using cotton buds. Finally, the filtered cells present on the lower side of the transwell inserts were immobile using 4 % PFA and marked using 0.1 % crystal violet. The cells were then visualized using a light microscope (model). The images were analysed using ImageJ software (version).

### Cytokine assessment:

The cytokine secreted by the cells was analyzed using the protocol available in the kit. Cells were seeded in  $1 \times 10^6$  in DMEM media for overnight in  $\text{CO}_2$  incubator at 37°C temperature and 95% humidity. Next cells, cells were exposed for the drug treatment for 24-hours and the cytokines was released into the culture medium. Supernatant was collected in eppendorfs and centrifuge at 6000 rpm at 4°C for 10 minutes. The cytokine was assessed as per the protocol provided by the ELISA kit (Progene Lab).

### Statistical analysis:

The results were calculated in form of Mean standard deviation. Comparison among control, and treated were analyzed by One-Way ANOVA using graph pad prism software. The significance of data has been recognized at  $p < 0.001$  level.

## Results and Discussion

## Morphological assessment of MCF-7 cells post treatment

MCF-7 cell line is extensively used in breast cancer research owing its unique properties and molecular profile. MCF-7, a secondary breast cancer cell line is HER2 negative and estrogen receptor (ER) positive, progesterone receptor positive which are characteristic features observed in luminal subtype breast cancers. Since, MCF-7 cells are responsive to estrogen, it is used as a model for estrogen-dependent breast cancers. Estrogen receptors present on MCF-7 cells enables researchers to investigate the role of estrogen and anti-estrogen treatments on growth and survival of breast cancer. The SEM images of MCF-7 cells from normal and treated groups shows significant morphological alterations.

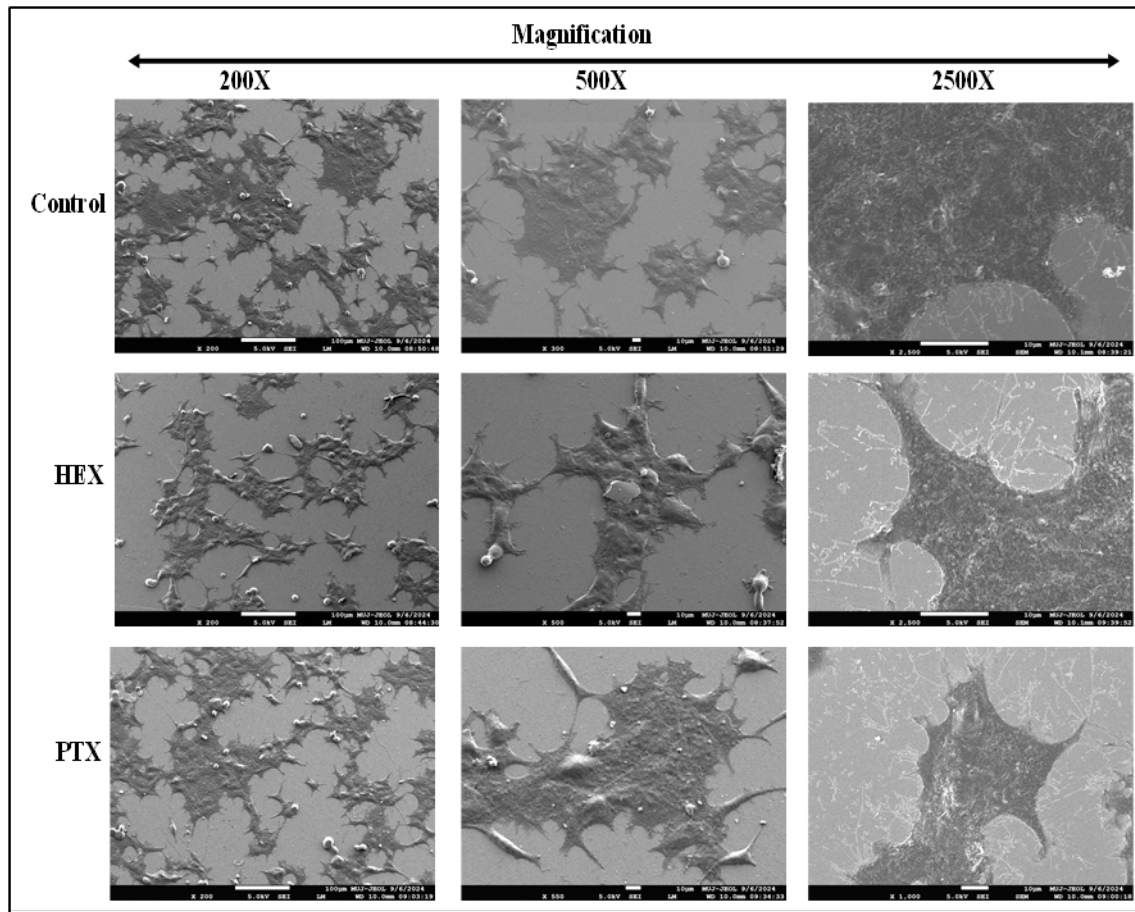


**Figure 2:** SEM image analysis of morphological alterations of MCF-7 cells of control, HEX treated MCF-7 and PTX treated MCF-7 cells.

The control cells had lot of tomenta on the cellular surface and had rounded appearance. After treatment with HEX, the cell surface shows white coloured perturbations that was a relevant marker for the HEX causing disintegration of the cell membrane. The images of PTX treatment cells were found to have more blebbing of the cell membrane. The shape of almost all the cells were altered and enhanced disintegration appeared at the cell edges. The white coloured lines were indicative of tubulin disassembly due to PTX treatment that also causes distortion of cell boundaries. At higher magnification, the control group retained the exact morphologies with sharp boundaries. Further, HEX treated group also showed distortion of cell shape.

#### PTX endorses migration and invasion of breast cancer cells

Taxanes and cycloheximide have been recognized as the keystones of chemotherapy in the managing of breast cancer metabolism. To examine the cytotoxicity of these two agents, first we determined

the half maximal inhibitory concentrations ( $IC_{50}$ ) of PTX and HEX by using dose-response cell viability curve. The  $IC_{50}$  values of PTX and HEX in MCF7 cells were  $8.56\mu\text{g}/\text{mL}$  and  $26.5\mu\text{g}/\text{mL}$ ; the  $IC_{50}$  calculated for PTX at 48 hrs was  $5.56\mu\text{g}/\text{mL}$ , for HEX it was  $18.36\mu\text{g}/\text{mL}$ , respectively.

MCF-7 cells were exposed to different PTX concentrations for 48 h, and cell viability was estimated using the MTT assay (Fig. 2A). The results suggested that that cell viability reduced significantly as the concentration of PTX increased ( $p < 0.05$ ). When the dose increases, the viability was found to be lower, as well as with increase in exposure time, the viability also reduced. Dose-dependent and time-dependent effects on the percentage viability was evaluated in MCF-7 cells. The percentage viability for HEX at 24 hours' time point was recorded as  $83.58209 \pm 0.231656$ ,  $76.97228 \pm 0.82705$ ,  $72.96375 \pm 0.626951$ ,  $70.1919 \pm 0.918464$  for  $12.5\mu\text{g}/\text{mL}$ ,  $25\mu\text{g}/\text{mL}$ ,  $50\mu\text{g}/\text{mL}$  and  $100\mu\text{g}/\text{mL}$ ,

respectively. For PTX percentage viability was recorded at  $60.18995 \pm 0.26907$ ,  $57.69687 \pm 0.755025$ ,  $49.8615 \pm 0.424018$ ,  $41.86783 \pm 0.115632$  for 12.5  $\mu\text{g}/\text{mL}$ , 25  $\mu\text{g}/\text{mL}$ , 50  $\mu\text{g}/\text{mL}$  and 100  $\mu\text{g}/\text{mL}$ , respectively. The percentage viability for PTX at 48 hours' time point was recorded as  $56.5032 \pm 0.878702$ ,  $45.07463 \pm 0.144147$ ,  $42.04691 \pm 0.832376$ ,  $39.06183 \pm 0.475185$  for 12.5  $\mu\text{g}/\text{mL}$ , 25  $\mu\text{g}/\text{mL}$ , 50  $\mu\text{g}/\text{mL}$  and 100  $\mu\text{g}/\text{mL}$  respectively. For HEX percentage viability was recorded at  $70.46524 \pm 0.164783$ ,  $68.29332 \pm 0.190928$ ,  $62.70749 \pm 0.014608$ ,  $56.31183 \pm 0.855378$  for 12.5  $\mu\text{g}/\text{mL}$ , 25  $\mu\text{g}/\text{mL}$ , 50  $\mu\text{g}/\text{mL}$  and 100  $\mu\text{g}/\text{mL}$  respectively. The percentage viability for PTX at 72 hours' time point was recorded as  $30.79774 \pm 0.505912$ ,  $28.23529 \pm 1.076763$ ,  $27.39726 \pm 0.105781$ ,  $19.5971 \pm 0.559407$  for 12.5  $\mu\text{g}/\text{mL}$ , 25  $\mu\text{g}/\text{mL}$ , 50  $\mu\text{g}/\text{mL}$  and 100  $\mu\text{g}/\text{mL}$  respectively. For HEX percentage viability was recorded at  $59.6755 \pm 0.255834$ ,  $39.35536 \pm 0.538382$ ,  $32.79613 \pm 0.111655$ ,  $29.36342 \pm 0.87843$  for 12.5  $\mu\text{g}/\text{mL}$ , 25  $\mu\text{g}/\text{mL}$ , 50  $\mu\text{g}/\text{mL}$  and 100  $\mu\text{g}/\text{mL}$  respectively.

	Concentration ( $\mu\text{g}/\text{mL}$ )	24 hours	48 hours	72 hours
HEX	12.5	$83.58209 \pm 0.231656$	$70.46524 \pm 0.164783$	$59.6755 \pm 0.255834$
	25.0	$76.97228 \pm 0.82705$	$68.29332 \pm 0.190928$	$39.35536 \pm 0.538382$
	50.0	$72.96375 \pm 0.626951$	$62.70749 \pm 0.014608$	$32.79613 \pm 0.111655$
	100.0	$70.1919 \pm 0.918464$	$56.31183 \pm 0.855378$	$29.36342 \pm 0.87843$
PTX	12.5	$60.18995 \pm 0.26907$	$56.5032 \pm 0.878702$	$30.79774 \pm 0.505912$
	25.0	$57.69687 \pm 0.755025$	$45.07463 \pm 0.144147$	$28.23529 \pm 1.076763$
	50.0	$49.8615 \pm 0.424018$	$42.04691 \pm 0.832376$	$27.39726 \pm 0.105781$
	100.0	$41.86783 \pm 0.115632$	$39.06183 \pm 0.475185$	$19.5971 \pm 0.559407$

**Table 1:** Dose and time dependent % cytotoxicity of MCF-7 post treatment with PTX and HEX estimated at 24-hour, 48 hour and 72 hours. N=3, Mean  $\pm$  S.D.

Migratory potential of cancer cells in the extracellular matrix is a cascade of channeling and dynamic changes in the cell-substrate adhesion, cytoskeleton, and the components of extracellular matrix. Migration was estimated by the scratch assay, which is a two-dimensional experimental design which is extremely reproductive, straight-forward, easy and cheap to perform in *in-vitro* models. The working principle involves the restoring capacity of cancer cells growing in monolayer morphology where the cells tried to restored any kind of disturbance either mechanical or else. This assay also describes the cancerous cell nature to make contact with each other and stay connected. Wound generation due to mechanical scratch and delayed in cell wound healing due to PTX and HEX treatment was observed. The wound healing rate/migration rate of the MCF-7 cells were calculated using ImageJ software.

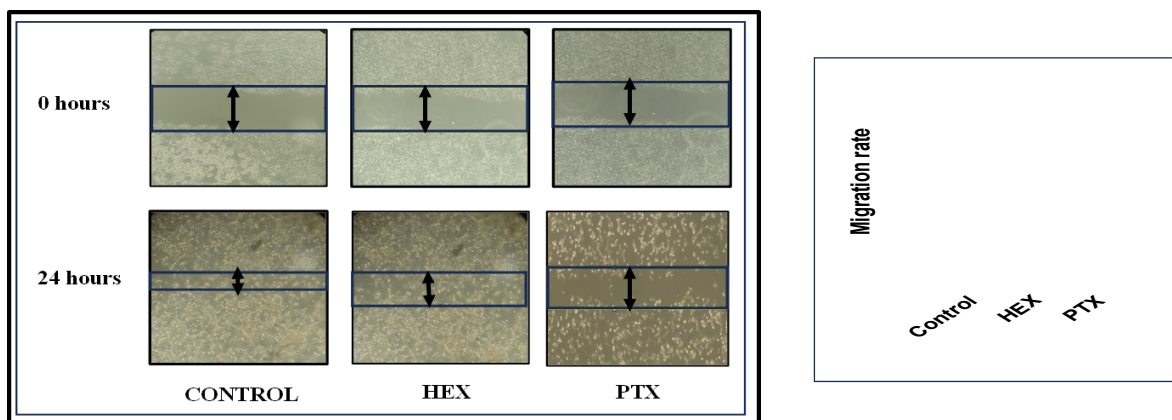


**Figure 3:** Scratch healing rate/migration rate of MCF-7 cells post exposure with PTX and HEX for 24 hours. n=3, mean  $\pm$  S.D., \*denotes significant difference between carboplatin concentration. \*\*\*p<0.01.

The scratch assay reveals that the untreated control group cells have their normal cell physiology which enabled them to divide faster and thereby healing the wound at extraordinary speed. The calculated migration rate was  $>60\%$ . Extraordinarily, the migration potential of breast cancer cells was reduced after subsequent treatment with PTX but not HEX (Figure 3). The HEX treated group causes delay in their protein metabolism as HEX was known protein inhibitor so delay was recorded in the wound. The calculated migration rate was calculated as  $<60\%$ . The PTX treated group shows that cells stop their cell division and hindered their mitosis rate, so the maximum delay was observed for migration. The calculated migration rate was calculated as  $>40\%$ . The migratory ability decreased after treatment with PTX when compared to the control group.

Next, we resolute the invasion of MCF-7 by an addition of matrigel matrix on upper layer of the transwell membrane to imitate the mechanism of extracellular matrix invasion and extravasation of breast cancer cells. Here, we checked whether PTX inhibits migratory potential of MCF-7 breast cancer cells.

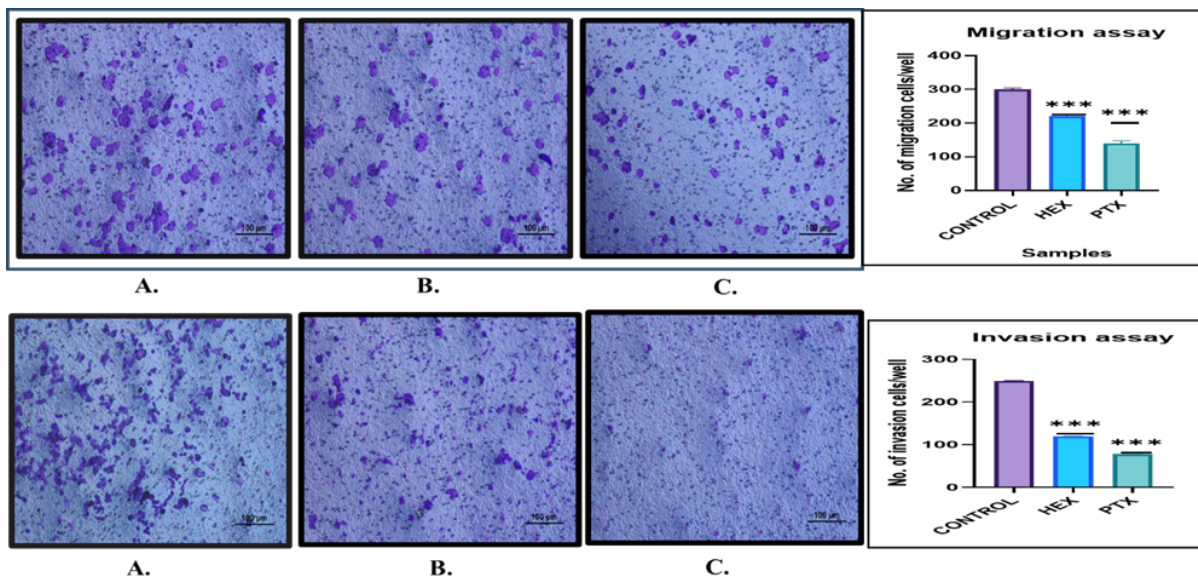


**Figure 4:** Cell migration and invasion assay performed using transwell. MCF-7 cells were treated with HEX and PTX for 24 hrs. Images were captured by inverted compound microscope at two-time intervals: 0-hours and 24-hours. The maximum healing was observed in untreated cells follow by HEX. And the PTX causes cell cycle restriction causing minimal healing even after 24 hours.

The untreated control indicated maximum invasion of cells. Around 30 % invasion rate was detected in the cells exposed with HEX. PTX treated cells caused oxidative stress that indicated low invasion rate (~09 %). In invasion assay maximum invasion in control group and minimal invasion in PTX treated group was observed. Reliable with the outcomes of the migration assay, the cell capacity to invade were 30% when related to control succeeding treatments with PTX and HEX, respectively (Figure 4).

Cancer cell on the process of metastasis firstly starts migration and invasion. Malignant cancer cells exploit their inherent migratory potential to conquer adjacent muscular and connective tissues, and eventually metastasize. Cell migration is entirely a channelizing cascade originated by the establishment of membrane flanges in comeback to wandering and chemotactic stimuli [20].

Inflammatory cytokines and chemokines are known to promote tumor cell survival and invasion; hence the pro-inflammatory and anti-inflammatory cytokine expression were estimated after 24 hours of PTX and/or HEX treatment. Treatment with a high concentration (30  $\mu$ M) of PTX arouses local release of tumor necrosis factor (TNF)- $\alpha$ , a potent apoptosis related cytokine marker, from animal model obtained peritoneal macrophage. In spite of its improbable clinical significance due to the supra-pharmacologic PTX upregulation has been necessary, this reflection still reinforces the conception that PTX has multiple effects on the cells. PTX is also shown to activate interleukin (IL)-10 in breast carcinoma cells. Graph represents PTX induced release of pro-inflammatory cytokine in the supernatant that triggers ROS generation further leading to death following early apoptosis pathway (under communication).

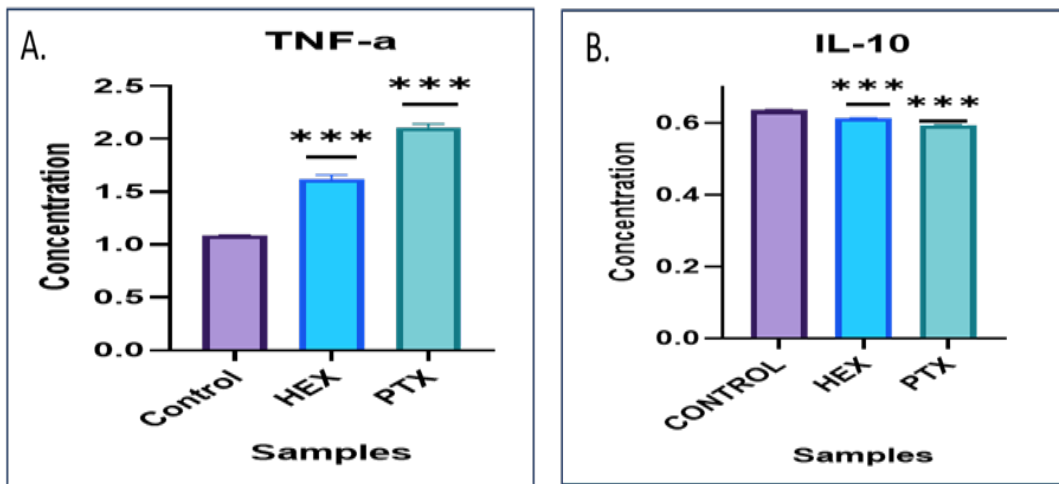


**Figure 5:** Cytokine assessment of the MCF-7 cells. [A] Indicates increased levels of pro-inflammatory cytokine- TNF- $\alpha$  [B] Reduced levels of anti-inflammatory cytokine IL-10.

It has been reported that TNF- $\alpha$  plays a central part in cancer initiation, proliferation, progression, metastasis, and EMT orientation by helping the damage of epithelial proteins and enhancing the mesenchymal proteins upregulation. PTX has been revealed to reduction tumor metastasis by enhancing TNF- $\alpha$  levels.

## Conclusion

In summary, we show here that PTX chemotherapy is the furthermost controlling natural invention offered to treat cancer ascites substantially increases the cell cytotoxicity. We report that PTX reduces the cell propagation, migration, and invasion of MCF-7 cells. PTX can modulate the consequence of immunotherapy by numerous mechanisms of accomplishment proceeded on to immune cells production and activation, so an important branch of immunomodulation therapeutics. Its leftovers uncertain whether PTX-induced inflammation can affect its chemotherapeutic potential when used with other drugs. However, the tumor immune process is intricate and cancer is tough to remedy completely. The role of PTX in tumor immunotherapy involvements desires to be further quantified.

**Competing Interests:** The authors have no conflicts of interest to declare.

**Acknowledgements:** Kriti Bhardwaj is thankful to DBT-JRF for their JRF fellowship grant.

## Authors' Contribution

**Conceptualization:** Kapinder, Anita K.Verma.

**Data curation:** Kriti Bhardwaj, Karishma Niveria, Vinay K.Singh

**Formal analysis:** Anita K.Verma. Karishma Niveria

**Funding acquisition:** Anita K.Verma

**Investigation:** Kriti Bhardwaj, Karishma Niveria

**Methodology:** Kriti Bhardwaj, Karishma Niveria.

**Project administration:** Anita K.Verma

**Resources:** Anita K.Verma

**Validation:** Anita K.Verma.

**Visualization:** Kriti Bhardwaj, Karishma Niveria.

**Writing—original draft:** Kriti Bhardwaj, Kapinder, Anita K.Verma

**Writing—review & editing:** Kapinder, Anita K.Verma, Kriti Bhardwaj.

## References

1. Wani MC, Taylor HL, Wall ME, Coggon P, McPhail AT (1971) Plant antitumor agents. VI. Isolation and structure of taxol, a novel antileukemic and antitumor agent from *Taxus brevifolia*. *J Am Chem Soc* 93: 2325-2327.
2. Shetty D, Zhang B, Fan C, Mo C, Lee BH, et al., (2019) Low dose of paclitaxel combined with XAV939 attenuates metastasis, angiogenesis and growth in breast cancer by suppressing Wnt signaling. *Cells* 8:892.
3. Xiaomeng F, Lei L, Jinghong A, Juan J, Qi Y, et al., (2020) Treatment with  $\beta$ -elemene combined with paclitaxel inhibits growth, migration, and invasion and induces apoptosis of ovarian cancer cells by activation of STAT-NF- $\kappa$ B pathway. *Braz J Med Biol Res* 53: e8885.
4. Li G, Xu D, Sun J, Zhao S, Zheng D (2020) Paclitaxel inhibits proliferation and invasion and promotes apoptosis of breast

cancer cells by blocking activation of the PI3K/AKT signaling pathway. *Adv Clin Exp Med* 29:1337-1345.

5. Zhang D, Sun L, Liu F, Ling G, Xiao L, et al., (2010) Low-dose paclitaxel ameliorates renal fibrosis in rat UUO model by inhibition of TGF- $\beta$ /Smad activity. *Lab Invest* 90:436-447.
6. Wang C, Song X, Li Y, Han F, Gao S, et al., (2013) Low-dose paclitaxel ameliorates pulmonary fibrosis by suppressing TGF- $\beta$ 1/Smad3 pathway via miR-140 upregulation. *PLoS One* 8: e70725.
7. Weaver BA (2014) How Taxol/paclitaxel kills cancer cells. *Mol Biol Cell* 25:2677-2681.
8. Zhang D, Yang R, Wang S, Dong Z (2014) Paclitaxel: new uses for an old drug. *Drug Des Devel Ther* 8:279-284.
9. Miao Y, Du Q, Zhang HG, Yuan Y, Zuo Y, et al., (2023) Cycloheximide (CHX) chase assay to examine protein half-life. *Bio Protoc* 13: e4690.
10. Binder C, Binder L, Kroemker M, Schulz M, Hiddemann W (1997) Influence of cycloheximide-mediated downregulation of glucose transport on TNF $\alpha$ -induced apoptosis. *Exp Cell Res* 236:223-230.
11. Sung H, Ferlay J, Siegel RL, Laversanne M, Soerjomataram I, et al., (2021) Global cancer statistics 2020: GLOBOCAN estimates of incidence and mortality worldwide for 36 cancers in 185 countries. *CA Cancer J Clin* 71:209-249.
12. Smolarz B, Nowak AZ, Romanowicz H (2022) Breast cancer—epidemiology, classification, pathogenesis and treatment (review of literature). *Cancers (Basel)* 14:2569.
13. Hanahan D, Weinberg RA (2011) Hallmarks of cancer: the next generation. *cell* 144:646-674.
14. McMillin DW, Negri JM, Mitsiades CS (2013) The role of tumour-stromal interactions in modifying drug response: challenges and opportunities. *Nat Rev Drug Discov* 12:217-228.
15. Greten FR, Grivennikov SI (2019) Inflammation and cancer: triggers, mechanisms, and consequences. *Immunity* 51:27-41.
16. Mantovani A, Allavena P, Sica A, Balkwill F (2008) Cancer-related inflammation. *Nature* 454:436-444.
17. Binnewies M, Roberts EW, Kersten K, Chan V, Fearon DF, et al., (2018) Understanding the tumor immune microenvironment (TIME) for effective therapy. *Nat Med* 24:541-550.
18. Todoric J, Antonucci L, Karin M (2016) Targeting inflammation in cancer prevention and therapy. *Cancer Prev Res (Phila)* 9:895-905.
19. Mittal D, Biswas L, Verma AK (2021) Redox resetting of cisplatin-resistant ovarian cancer cells by cisplatin-encapsulated nanostructured lipid carriers. *Nanomedicine (Lond)* 16:979-995.
20. Liu CL, Chen MJ, Lin JC, Lin CH, Huang WC, et al., (2019) Doxorubicin promotes migration and invasion of breast cancer cells through the upregulation of the RhoA/MLC pathway. *J Breast Cancer* 22:185-195.